Available online at www.sciencedirect.com
ScienceDirect
Polymer 48 (2007) 6554–6564
polymer
www.elsevier.com/locate/polymer

Development and characterization of photopolymerizable biodegradable materials from PEG–PLA–PEG block macromonomers

Jason D. Clapper [a], Jessica M. Skeie [b], Robert F. Mullins [b], C. Allan Guymon [a,*]

[a] Department of Chemical and Biochemical Engineering, The University of Iowa, Iowa City, IA, USA
[b] Department of Ophthalmology and Visual Sciences, The University of Iowa, Carver College of Medicine, Iowa City, IA, USA

Received 30 April 2007; received in revised form 2 August 2007; accepted 3 August 2007
Available online 15 August 2007

Abstract

As tissue engineering and drug delivery applications increase in both number and complexity, the demand for new synthetic biocompatible polymers with precisely tailored properties grows accordingly. Block copolymers are a particularly promising biomaterial as the physical and physiological properties of these polymers can be closely controlled through manipulation of the type and organization of the blocks in the polymer's backbone. In this work, poly(ethylene glycol) (PEG) and poly(lactic acid) (PLA) were incorporated into PEG–PLA–PEG block macromonomers with (meth)acrylate functionality to form photopolymerizable, highly cross-linked polymers for potential use in a variety of biomedical applications. Simply by directing the PLA:PEG ratio in these macromonomers, the hydrophobicity, physical behavior, degradation, and biocompatibility of the resulting polymer were controlled. Specifically, it was found that by increasing the PLA:PEG ratio, the degree of water uptake and the mechanical strength of the material is significantly decreased, while the glass transition temperature and degradation of the PEG–PLA polymers are delayed. Additionally, the biocompatibility of the PEG–PLA polymers is significantly influenced by the chemical composition of the material as increased PLA generally yields greater cell compatibility. By demonstrating the versatility of the photopolymerizable PEG–PLA polymers, the results of this study indicate that these materials have the potential to serve as a synthetic biomaterial platform, in which the properties of the polymer can be tailored to a variety of tissue engineering or drug delivery applications.

Keywords: Photopolymerization; Biodegradable; Biomaterial

1. Introduction

Biomaterials for tissue engineering or drug delivery have seen numerous advances in recent years as researchers continue to develop and modify polymeric materials to meet the demanding needs of these biomedical applications. Towards this end, many types of synthetic and natural polymers have been synthesized and employed as drug delivery vehicles or tissue scaffolding, roles that typically require precise and controllable polymer properties for successful function [1–4]. Degradable analogs of these biopolymers have received particular attention by reducing the need for device removal surgery. Recent results have demonstrated that an appropriate breakdown of the synthetic biomaterial allows for improved healing and increased tissue function, or a highly controlled release of large molecular weight biomolecules compared to non-degradable hydrogel constructs [4–6]. In addition to degradation, the ability to tune the physical properties of degradable polymers is an integral part of biopolymer design as properties such as water content, permeability, and mechanical strength have been shown to influence drug release, as well as cellular growth and function, critical parameters for successful tissue engineering or delivery applications [7–10].

In the continually expanding library of natural and synthetic polymers available for biomedical applications, block copolymers of poly(ethylene glycol) (PEG) and poly(lactic acid) (PLA) have emerged as one of the more promising biodegradable materials due to their highly controllable chemical

* Corresponding author. Tel.: +1 319 335 5015.
E-mail address: allan-guymon@uiowa.edu (C.A. Guymon).

0032-3861/$ - see front matter © 2007 Elsevier Ltd. All rights reserved.
doi:10.1016/j.polymer.2007.08.023

and physical properties [11–13]. Early work by Hubbell documented the versatility of these materials by showing drastically different polymer properties simply by changing the size of the PEG and PLA blocks in the polymer network [14]. This work also demonstrated the specific roles of the PEG and PLA blocks in the biopolymer as PEG groups add hydrophilicity and bring water into the network, while PLA blocks (less hydrophilic than PEG) enable the biodegradability of the material with their hydrolytically cleavable ester moieties. This simple axiom can be expanded as further studies have shown that blending polymer formulations with PLA increases mechanical strength, glass transition temperature, and cell biocompatibility over simple PEG hydrogel systems [15,16]. In addition, the presence of PEG in the copolymer aids in the control of cell–biomaterial interactions by preventing non-specific protein binding, a drawback of traditional PLA biomaterials [11].

The general structure of photopolymerizable PEG–PLAs studied to date are comprised primarily of a large central PEG chain flanked by PLA blocks of varying size, end-capped with functional vinyl groups to allow cross-linking of the macromonomers. Typically these macromonomers are large ($MW > 5000$) leading to networks with a relatively low cross-link density, high degree of network swelling in water, and low mechanical properties [14,17,18]. In this study, we have explored the synthesis of lower molecular weight photopolymerizable PEG–PLA–PEG macromonomers ($MW < 2000$) using a synthesis scheme that results in a new arrangement of the PEG and PLA blocks in the monomer. By reversing the traditional order of the blocks, placing the hydrophobic PLA in the middle of the macromonomer, hydrophilic PEG blocks flanking the PLA, and capping the macromonomer with (meth)acrylate functionality, a new PEG–PLA photopolymerizable macromonomer is formed. It is expected that the reverse PEG–PLA–PEG block orientation will change the monomer and/or polymer behavior in a number of potential applications including drug loading and polymer interactions for the fabrication of drug delivery polymer vehicles, compatibility in multi-component biodegradable composites, or even the ability to template the biodegradable monomer within a nanostructured lyotropic liquid crystal [19,20]. In addition, the use of relatively small PEG and PLA blocks as starting materials in this study allows for a simple pathway to fabricate PEG–PLA–PEG networks that are highly cross-linked with good mechanical integrity and material properties that may be directly controlled through the manipulation of the PEG:PLA block ratio.

The current synthesis of the PEG–PLA–PEG block macromonomers expands on a scheme first proposed by Jeong et al. in which low molecular weight, non-reactive block macromonomers were developed for drug delivery applications. The thermo-sensitive PEG–PLA–PEG monomers synthesized by Jeong et al. gel in aqueous solution by forming aggregates of micelles through hydrogen bonding [21]. In the present work, reactive (meth)acrylates groups were added to the PEG–PLA–PEG molecules leading to the formation of a network with physical cross-links that are not soluble until hydrolytically cleaved by aqueous solution. Cross-linking serves not only to increase the network's mechanical properties, but also plays a role in controlling water uptake, influencing permeability, and regulating the breakdown of the network. Previous work has demonstrated that the physical properties of biopolymers are much easier to control in cross-linked networks due to the fact that manipulation of the matrix cross-link density directly influences such material properties as mechanical strength, swelling, transport behavior, and degradation [17,22–24], as well as physiological properties such as cell health, proliferation, and cell function [25,26].

The work described herein characterizes the physical properties and polymerization behavior of the newly synthesized biodegradable PEG–PLA–PEG cross-linked materials, demonstrating the property modulation that can be achieved in this system through simple polymer chemistry. Specifically, the macromonomer's molecular weight, block composition, and reactive functional groups were varied while measuring the key physical parameters of the resulting polymer network, including water uptake, mechanical properties, degradation rate, polymerization behavior, and biocompatibility. This paper aims to understand the relationships between the designed structure and chemistry of the macromonomer and the resulting behavior of the synthesized biomaterial in an effort to enable the precise tailoring of its physical properties to a number of current and future biomedical applications including drug delivery, biodegradable composite formulation, and tissue engineering bioscaffold design.

2. Experimental

2.1. Materials

Poly(ethylene glycol) acrylate (PEGA, MW 375, Aldrich) and poly(ethylene glycol) monomethacrylate (PEGMA, MW 400, Polysciences) were dried by azeotropic distillation with benzene. DL-lactide (MW 144, Polysciences) was recrystallized in hexanes from ethyl acetate prior to use. Dulbecco's phosphated buffer saline solution (Aldrich) was mixed with 10 L of distilled water to obtain a pH of 7.4 (9.6 g/L of water). Hexamethylene diisocyanate (Aldrich), stannous octoate (Aldrich), the photoinitiator 1-hydroxycyclohexyl phenyl ketone (Irgacure 184, Ciba), and all other solvents were obtained and used without further purification.

2.2. Methods

The synthesis scheme for the diacrylate PEG–PLA–PEG macromonomer with a 3.5:*n* molar ratio of EG (ethylene glycol repeat groups) to LA (lactic repeat groups), named PL(*n*)PDA, is shown in Fig. 1. Briefly, for the synthesis of PL2PDA, 25 g of dry PEGA, 19.2 g DL-lactide (2 mol DL-lactide/mol PEGA), and 60 ml of toluene were charged to a 250-ml round bottom flask under an argon atmosphere. The reaction vessel, fitted with a condenser, was stirred at reflux temperatures for the reaction toluene solvent (110 °C) for 0.5 h

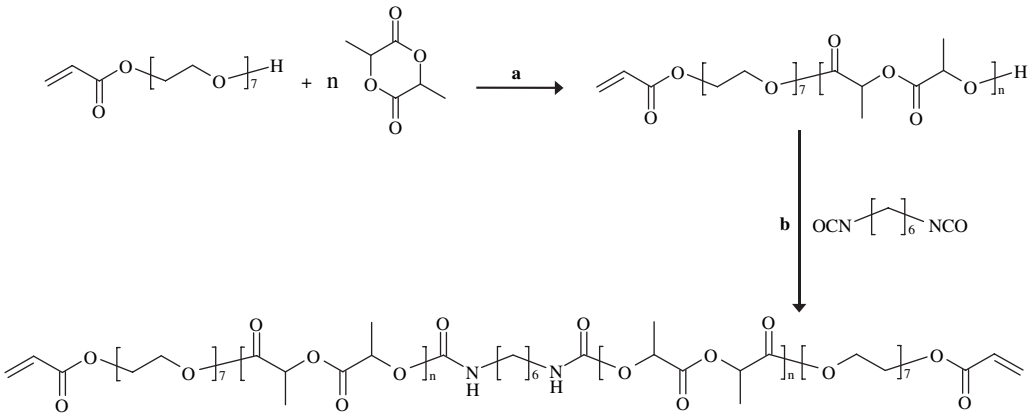

Fig. 1. Synthesis scheme of PL(*n*)PDA monomer in a two step reaction involving the ring opening addition of lactide to PEGA (a), and the coupling of the PEGA–PLA blocks using a diisocyanate linker to make the photopolymerizable PEG–PLA–PEG block macromonomer (b).

to let the lactide melt into solution. Two hundred milligrams of stannous octoate was added to the flask and the solution was stirred for 6 h at reflux conditions and cooled to 60 °C. Hexamethylene diisocyanate (5.6 g) was slowly added to the flask to couple the diblock PEG–PLA. No additional catalyst was added for the isocyanate and alcohol reaction. The reaction vessel was stirred for 12 h at 60 °C, followed by 6 h at reflux temperatures. After cooling to room temperature, the monomer product in the reaction vessel was extracted using hexane (1×400 ml), a 1:1 mixture of petroleum ether and ethyl ether (1×400 ml), and pure ethyl ether (2×400 ml). The resulting product, a viscous semi-clear liquid, was then dried overnight in a vacuum oven. Typical yields for this synthesis on a mass basis were 70–85% with the lower yields resulting from the more viscous PL3PDA monomers due to recovery issues. The synthesis scheme for the dimethacrylate version of the PEG–PLA–PEG block monomer is identical except for the vinyl group on the precursor PEG chain and the term DMA to represent dimethacrylated monomers.

2.3. Characterization of PLPDA block monomers

IR analysis of the synthesized block monomers was accomplished using a Thermo Electron Nexus 670 Fourier transform infrared spectrometer (FTIR) with ATR accessory. The detector of the FTIR was cooled with liquid nitrogen and the instrument was purged with nitrogen gas to suppress noise from carbon dioxide and water vapor in the environment. For each run, approximately 10 μL of monomer solution was placed on the ATR crystal and 64 scans were taken to create a transmission spectrum. ^{1}H NMR spectra were obtained using a Bruker Avance 300 probe using 16 scans per sample. For analysis approximately 25 mg of product was dissolved in 0.5 mL of deuterated chloroform.

2.4. UV polymerization characterization

For polymerization characterization, 75 and 40 wt% solutions of the block macromonomer in ethylene glycol diacetate (used to prevent solvent evaporation from convoluting the polymerization results) were mixed thoroughly. Photoinitiator (0.75 wt%) was added to each solution. The photopolymerization reaction was investigated using both photo-differential scanning calorimetry (PDSC) and real-time infrared spectroscopy (RTIR). For PDSC, a Perkin–Elmer differential scanning calorimeter was fitted with a medium pressure UV arc lamp (ACE Glass) to initiate polymerization. A 365 nm filter was used to control the emission spectrum and light intensity (1.8 mW/cm^2). The polymerization rate was determined as a function of time using the exotherm from the reaction and previously defined methods [27].

A Thermo Electron Nexus 670 Fourier transform infrared spectrometer (FTIR) was modified to allow for real-time monitoring of photopolymerizations. Photopolymerization was initiated using a high-pressure mercury arc lamp (Exfo Acticure 4000) using 365 nm light (1.8 mw/cm^2). The double bond conversion of the monomer sample was calculated using the height of the IR peak of the (meth)acrylate functional group (810 cm^{-1}) and previously defined methods [27].

For physical property experiments, 75 and 40 wt% solutions of the block macromonomers in ethanol were mixed thoroughly for 1 h prior to polymerization. Photoinitiator (0.75 wt%) was added to each solution. Bulk polymerizations of the synthesized monomers were not attempted in this study due to the high viscosity of the monomer preventing adequate dissolution and uniform mixing of the photoinitiator. Polymer squares were made by pouring 1 ml of monomer solution into a nylon mold with $2 \times 2 \times 0.25$ cm troughs. The mold was placed in a nitrogen purged box for 10 min and then irradiated using a 365 nm UV light source (1.8 mW/cm^2). Disks were punched from these square polymer samples for both swelling and modulus tests.

2.5. Mechanical and swelling characterization

Water absorption was measured gravimetrically by immersing dried polymer disks into 37 °C PBS solution and measuring water uptake at given intervals. Swelling measurements were taken by removing the gel from solution, patting the surface dry, and then recording the mass of the hydrated polymer.

Equilibrium water absorption was determined once the mass of the hydrated sample did not change significantly as a function of overall swell time and was calculated using previously defined methods [28]. For swelling and all additional tests below, three polymer samples were made for all formulations to obtain a standard deviation for each resulting data point, represented by error bars in the reported figures.

Dynamic mechanical analysis (DMA, TA instruments Q800 series) was used to determine the compressive modulus of PLPDA samples in both the dehydrated and swollen state. Dehydrated disks were dried post-polymerization. For the hydrated modulus tests, samples were incubated in 37 °C water for 24 h prior to the compressive test. Disk shaped samples were placed on the compressive clamp of the DMA and compressed to approximately 90–95% of their original height. Compressive modulus was determined using stress/strain curves from the DMA runs.

DMA was also utilized to determine the glass transition temperature (T_g) of the PEG–PLA photopolymerized materials. Bar shaped samples of each material were polymerized using monomer formulations of 75 and 40 wt% macromonomer in ethanol. The samples were swelled in ethanol to remove any unpolymerized macromonomer, and then dried overnight before testing. Samples were placed in the single cantilever clamp on the DMA and oscillated at 1 Hz, using a deformation strain of 0.05%, as the temperature was slowly ramped from −90 to 60 °C. Storage modulus and tan δ were plotted vs. temperature to determine the T_g of the material, the temperature corresponding to the peak in the tan δ/temperature profile.

2.6. Degradation analysis

The degradation profile of each polymeric material was determined by creating 40 ($1 \times 1 \times 0.25$ cm) squares. Dried samples were weighed and immersed in approximately 20 ml of PBS solution in individual vials kept at 37 °C. Samples were removed at designated times and weighed in both the hydrated and dried states. Triplicate samples were removed at each time point to gauge the variability in the degrading samples, represented by error bars on the mass loss and water uptake figures. Mass loss and water uptake were recorded as a function of time. The pH of each sample solution was also tracked and all vials for a particular material were replaced with new PBS if the pH dropped below 6.4 on a recorded sample.

2.7. Cell biocompatibility

Cell compatibility of the generated polymers was investigated using a lactate dehydrogenase (LDH) ELISA cytotoxicity detection kit (Roche Diagnostics Corp.). The mouse endothelial cell line C166 (American Type Culture Collection, Manassas, VA) was grown to confluency (1 week) in a 24-well TPS plate in Dulbecco's Modified Eagle Glucose Rich Medium supplemented with 10% Bovine Serum, 1% Penicillin, and 0.1% Amphotericin B. Polymer sample cubes ($2 \times 2 \times 2$ mm) were placed in the culture medium on top of the monolayer of healthy endothelial cells. After 1 week of incubation, the medium was analyzed using the LDH ELISA and a Thermo Multiskan plate reader to determine the absorbance of the medium at 492 nm. Controls were established using wells with cells and no polymer (baseline cell death under these conditions), wells with polymer and no cells (baseline absorbance), and wells with cells lysed in 1% Triton X-100 to quantify 100% cell death. Additional controls were performed using the ELISA assay to compare a solution of lysed cell medium and PBS with degrading polymer (LDH with polymer degradation products) to a solution of lysed cell medium and PBS (LDH without polymer degradation products). Again, triplicate sets were performed for all samples and controls. Relative cell death (RCD) was established using Eq. (1) below in which T is the absorbance recorded for 100% cell death, B is the baseline absorbance (no cell activity), and R is the absorbance for the given run.

$$\mathrm{RCD} = \frac{R - B}{T - B} \times 100\% \tag{1}$$

3. Results and discussion

Synthetic polymers are often selected for use as biological applications due to the high degree of control over the physical properties and behavior that is accessible through chemical manipulation. Previous research encompasses a wide spectrum of methods to tailor and control the physical and biological properties of synthetic polymers including bulk chemistry, cross-link density, surface chemistry, and degradation mechanisms to name a few [6,8,25,29]. In this work, PEG–PLA–PEG block macromonomers were synthesized in which the chemistry of the biomacromonomer was varied simply by changing the block composition of the macromonomer. The resulting physical behavior of the PEG–PLA–PEG cross-linked materials was examined as a function of macromonomer chemistry to determine the effect of polymer structure and chemistry on properties such as network swelling, mechanical properties, degradation rate, glass transition temperature, and biocompatibility. By characterizing the newly synthesized biomaterials, this study expects to expand their use in such applications as drug delivery vehicles, multicomponent biocomposites, tissue engineering scaffolds, or nanostructured biopolymer systems.

3.1. Synthesis of PEG–PLA–PEG block monomers

To investigate the relationships between the designed chemistry of the PEG–PLA–PEG macromonomers and their physical behavior, (meth)acrylated macromonomers were synthesized with varying ratios of PEG and PLA blocks. Although the functional vinyl groups of the PEG–PLA–PEG macromonomers allow the material to form a cross-linked network, the chemical structure between the functional groups is expected to determine the physical behavior of these materials. Table 1

Table 1
Synthesized PEG–PLA–PEG acrylated macromonomers[a]

Polymer	EG:LA ratio	Hydrophilic:hydrophobic MW	Total MW
PL1PDA	7:2	3:2	1200
PL2PDA	7:4	1:1	1500
PL3PDA	7:6	3:4	1800

[a] The name of the monomer, the ratio of ethylene glycol (EG) to lactide (LA) repeat units, the expected hydrophilicity ratio based on molecular weight including the central hexamethylene chain, and the approximate molecular weight of each macromonomer are listed.

describes the chemical structure of the novel PEG–PLA–PEG macromonomers. In Table 1, PL2PDA indicates that a 2:1 ratio of DL-lactide to PEGA (acrylate) was used in the synthesis of this material resulting in a 4:7 ratio of lactic acid (LA) to ethylene glycol (EG) blocks between vinyl functional groups. The overall hydrophilicity of the material, depicted by the ratio of hydrophilic to hydrophobic molecular weight in the macromonomer, is expected to have an impact on the swelling and degradation of these materials in aqueous solutions. In addition, the total molecular weight of the macromonomer will directly influence the distance between cross-linking sections (i.e. cross-link density) and should have a dramatic effect on the physical and physiological behavior of these materials. Methacrylated analogs of the materials in Table 1 are chemically similar to the acrylates shown, apart from the methacrylate vinyl functionality, and are represented by the code PLPDMA in all further discussion. Although both methacrylate and acrylate functional macromonomers were synthesized, the only direct comparison between the two reported here is in the kinetic polymerization analysis. The remainder of this study reports only the physical property analysis of the acrylate version of each PEG–PLA–PEG macromonomer as there was little difference between the swelling, modulus, and degradation rate of the methacrylate and acrylate analogs. Rather the significant property changes occurred as the PEG–PLA block chemistry between the vinyl functional groups was varied.

The syntheses of the PLPDA and PLPDMA macromonomers were confirmed using both ^{1}H NMR and FTIR spectroscopy. Analysis of ^{1}H NMR spectroscopy showed the appearance of poly(lactic acid) protons at 1.5 and 5.2 ppm as well as a shift in the PEG methylene protons (4.2 ppm) immediately adjacent to the PEG–PLA joint confirming the addition of lactide to the hydroxy terminated PEGA. Coupling of the PEG–PLA molecules was observed with the appearance of the urethane linkage proton (–NH–) at approximately 2.5 ppm. Throughout the synthesis, vinyl protons remained intact with resonances at 5.8, 6.1, and 6.4 ppm. FTIR spectra for both PEGA and synthesized PL2PDA were used to track the macromonomer synthesis as shown in Fig. 2. The acrylate stretch (a) at 1640 cm^{-1} in both the PEGA and PL2PDA spectrum confirmed that acrylate groups remained intact throughout the synthesis. The addition of lactide to the PEGA was observed by the growth in the ester stretch (b) at 1750 cm^{-1} and the appearance of two peaks in this wave number range, showing contributions of both the ester groups adjacent to the acrylate and the ester groups in the added poly(lactic acid) blocks. Finally, the coupling of the PEG–PLA molecules using hexamethylene was traced by the disappearance of the PEGA hydroxyl peak (c) at 3500 cm^{-1} and the appearance of the urethane NH stretch (d) at 3350 cm^{-1}.

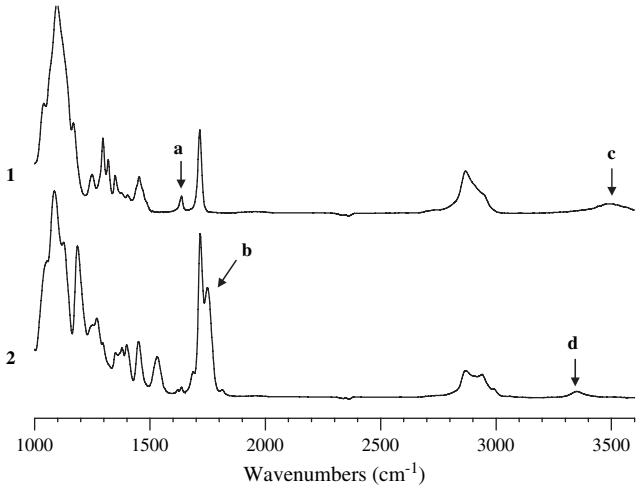

Fig. 2. FTIR spectrum of (1) precursor poly(ethylene glycol) acrylate (PEGA) and (2) synthesized PL2PDA, with spectrum peaks for the acrylate peak at 1640 cm^{-1} (a), the second ester stretch from the PLA at 1760 cm^{-1} (b), the PEGA hydroxy peak at 3500 cm^{-1} (c), and the urethane linkage at 3350 cm^{-1} (d).

3.2. Polymerization characterization

The polymerization of the functionalized macromonomers was observed using both photo-DSC and real-time IR methods examining the polymerization rate and the extent of conversion of (meth)acrylate vinyl groups. Though little divergence in the rate and extent of conversion was observed as the macromonomer lactide content was increased, significant variances in terms of polymerization rate were observed between the acrylate and methacrylate versions of the PLP macromonomers. Fig. 3 displays the polymerization profiles of PL2PDA and PL2PDMA taken using both P-DSC (Fig. 3A) and RTIR (Fig. 3B) methods. For both instruments, a definite rate enhancement is observed with the acrylated monomer over the methacrylated monomer. This trend has been well documented for various commercially available acrylate and methacrylate monomers in previous work, and is typically attributed to the steric hindrance of the methyl moiety on the methacrylate vinyl group [30,31]. Specifically, from Fig. 3A, the maximum rate of polymerization of the acrylate macromonomer is approximately seven times faster than the methacrylate version.

Fig. 3B also demonstrates the high degree of conversion for these monomers (typically above 90%), as well as the rapid nature of the photopolymerization reaction, in which most (>80%) of the reaction is complete within the first minute of irradiation. A high degree of conversion has both physical and physiological implications as unreacted monomer from low conversions can act as a plasticizer, compromising the

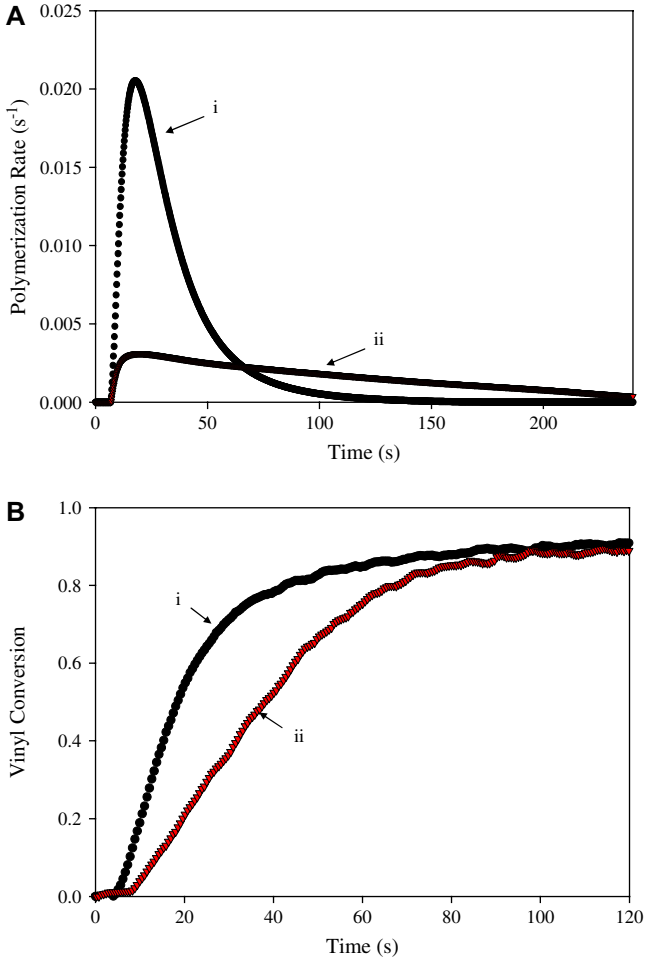

Fig. 3. (A) P-DSC polymerization profiles showing the rate of polymerization vs. time and (B) RTIR polymerization profiles describing the double bond conversion vs. time for acrylated PL2PDA (i), and methacrylated PL2PDMA (ii). All polymerizations were initiated with UV irradiation at time 0.

mechanical strength of the material. In addition, low conversions potentially decrease the biocompatibility of the polymer by retaining unreacted vinyl groups in the system [32].

3.3. Network swelling

The overall hydrophobicity of the PLPDA materials, a function of their lactide content (Table 1), is expected to heavily influence the degree of water uptake in these systems. To explore this relationship, PL1PDA, PL2PDA, and PL3PDA materials were photopolymerized from monomer solutions with both 75 and 40 wt% macromonomer in ethanol. Fig. 4 demonstrates a linear decrease in the initial water uptake of the system as the lactide content of the macromonomer is increased. Previous work and modeling have thoroughly characterized the swelling of cross-linked hydrogel networks showing that the degree of water uptake is dependent on two primary matrix characteristics; cross-linking density and the interaction between the polymer and solvent [33]. Network swelling theory predicts that as macromonomer content in the monomer formulation decreases, lowering the cross-link density of the

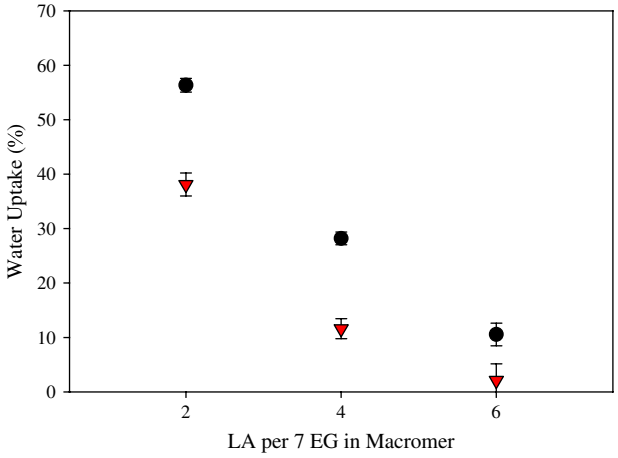

Fig. 4. Equilibrium water uptake of PLPDA materials as monomer lactide content is increased relative to the EG (ethylene glycol) content. Equilibrium swelling was investigated for macromonomer concentrations of 40 wt% (●) and 75 wt% (▼) in the pre-polymerization formulations.

polymerized network, the potential swelling of the material will increase due to increased void space in the polymer and a weakening of the retractile forces holding the network together. This relationship is evident in Fig. 4, as the PLPDA materials polymerized in a 40 wt% solution, that are expected to have a lower cross-linking density, swell consistently 10–20% more than the materials polymerized in a 75 wt% solution of the same monomer.

Within one macromonomer loading (e.g. 75 wt%), the observed swelling decreases almost 40% with increased lactide content even though the longer lactide chains in these macromonomers will effectively decrease the overall cross-link density of the network. In this case, the chemistry or hydrophobicity from increased lactide content of the macromonomer dictates the interaction between the polymer and water and is the dominant factor, influencing the swelling behavior of the PLPDA materials. This trend is also evident within the 40 wt% monomer solutions in which the more hydrophobic materials (i.e. PL2PDA and PL3PDA) again swell approximately 50% less than the PL1PDA networks. Thus, through simple manipulation of the PEG:PLA ratio and macromonomer concentration, a great deal of control over the degree of water uptake in the PLPDA materials is realized.

3.4. Mechanical property analysis

PLPDAs with increasing lactide content, polymerized with both 40 and 75 wt% macromonomer concentrations, were investigated to determine the influence of cross-link density, block composition, and macromonomer size on the compressive modulus of these materials. Furthermore, by testing the modulus of samples in both hydrated and dry states, the influence of swelling on the modulus of the network could also be determined. Fig. 5 shows the hydrated and dehydrated compressive modulus of PLPDA materials with increasing macromonomer lactide content. As expected, by removing the water from each network, the modulus of the dehydrated material is

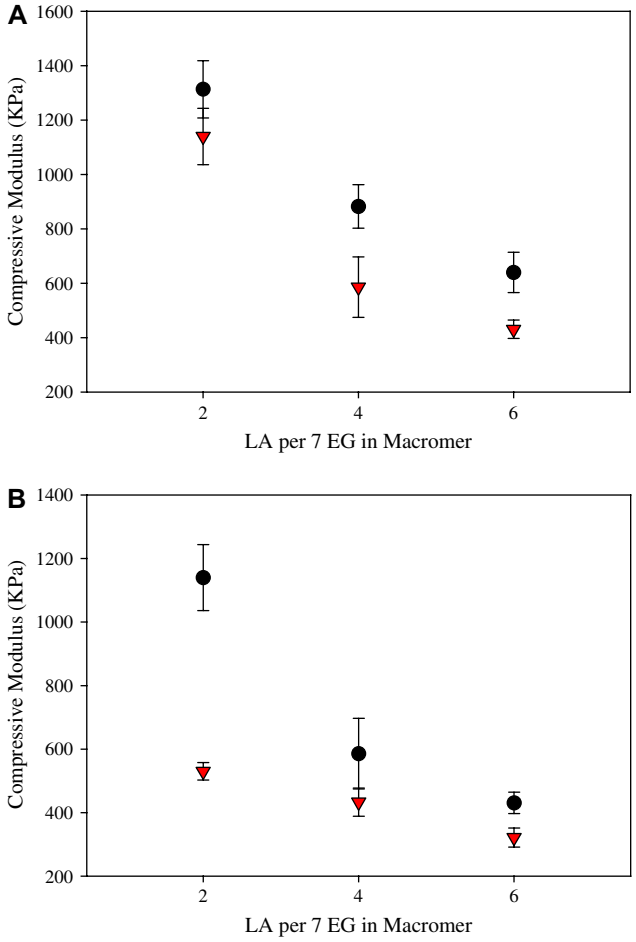

Fig. 5. Compressive modulus of PLPDA materials polymerized with both (A) 75 wt% and (B) 40 wt% macromonomer in the pre-polymerized formulations. Samples were compressed in both the dehydrated (●) and swollen state (▼).

consistently greater than the hydrated samples for the same lactide content. Furthermore, the observed differences between dry and swollen modulus is the greatest for 40 wt% PL1PDA gel which exhibits the highest degree of water uptake. Due to the amount of water in the swollen gel, a 600 kPa (45%) drop in modulus from the dehydrated value is observed for the 40 wt% macromonomer sample. On the other hand, the gap between wet and dry modulus is much closer for the low swelling 40 wt% PL3PDA material with a drop of only 100 kPa or 25% (Fig. 5B).

It is also observed in Fig. 5 that as the degree of lactide per macromonomer is increased from 2 to 6, the modulus decreases approximately 700 kPa for both the dehydrated 75 wt% macromonomer samples and the dehydrated 40 wt% macromonomer materials. The decrease in modulus with lactide content is unexpected given the earlier result in which a decrease in swelling with increased lactide was recorded (Fig. 4). Generally, a decrease in water uptake will serve to increase the modulus of a hydrogel network. However, as lactide content is increased and the size of the macromonomer increases, a decrease in cross-linking density is anticipated that would directly lead to a drop in the mechanical strength of the system [23]. The relationship between modulus, cross-link density, and lactide content can be observed in Fig. 5, in which the modulus of the 75 and 40 wt% macromonomer loaded PLPDA materials decreases 45 and 60%, respectively, with increased lactide content and macromonomer size. The correlation between cross-link density and modulus is also evident by comparing Fig. 5a and b. As the macromonomer content is diluted from 75 to 40 wt% and the cross-link density is consequently decreased, there is an average drop of 275 kPa in the compressive modulus of both the hydrated and dehydrated PLPDA samples. Thus, in regard to the mechanical properties of the PLPDA materials, it is evident that the polymer cross-link density is the dominant factor governing the mechanical properties of the biomaterial.

3.5. Glass transition temperature

Due to the vast differences in thermo-mechanical properties of cross-linked poly(ethylene glycol) and poly(lactic acid), the thermo-mechanical properties of the block macromonomers synthesized from PEG and PLA were investigated to assess the contributions from each block constituent to the properties of the copolymerized network. Dynamic mechanical analysis was used to determine the glass transition temperatures (T_g) of each of the three PLPDA materials, as well as to observe subtle differences in the network that may arise from the varying lactide in the backbone of each macromonomer. Fig. 6 displays the tan δ/temperature profiles for PL1PDA, PL2PDA, and PL3PDA. The peak of the tan δ/temperature profile is often recognized as the T_g of that material [34].

The range of T_g reported for cross-linked poly(ethylene glycol) with similar molecular weight to the synthesized macromonomers is approximately −40 °C to −60 °C [16,35]. Alternatively, the reported T_g for poly(lactic acid) of similar molecular weight is approximately 30 °C to 50 °C [16]. From Fig. 6, it is observed that the T_g of the biomaterials comprised of both PEG and PLA, respectively, fall between the T_g's of pure cross-linked PEG and PLA. This result is anticipated due to the fact that each PLPDA material contains

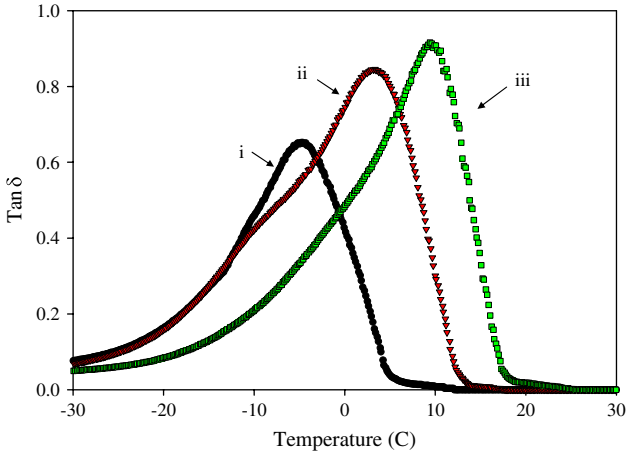

Fig. 6. Tan δ vs. temperature profiles taken for PL1PDA (i), PL2PDA (ii), and PL3PDA (iii) photopolymerized materials.

both PEG and PLA, and PL2PDA in particular possesses an approximate equal amount of the two in this monomer (Table 1). In addition, the intermediate T_g range for the PLPDA materials (−6, 3, and 9 °C) suggests that both the PEG and PLA segments of the block macromonomers contribute additively to the thermo-mechanical properties of the fabricated network.

3.6. Degradation and transient swelling

In addition to the initial swelling and mechanical assessment of the PLPDA biomaterials, the degradation behavior of these polymers was studied to determine the rate at which these cross-linked networks breakdown under physiological conditions. The swelling of the PLPDA materials was also tracked over time as this will directly impact degradation due to the breakdown mechanism of the PLPDA networks, i.e. the hydrolysis of ester bonds by water. Fig. 7A shows the mass loss over time of PLPDA networks with increasing PLA content in the macromonomer, while Fig. 7B describes the transient swelling behavior of these materials. In the first half of the degradation profile of each PLPDA material, the rate of mass loss seems to be determined by the hydrophobicity of the network with the more hydrophilic PL1PDA reaching 50% mass loss at day 33, while the hydrophobic PL3PDA material reaches 50% mass loss at day 70. The relationships between hydrophilicity, swelling, and degradation are shown in the swelling profiles of these materials (Fig. 7B) as the more hydrophilic PL1PDA polymer initially swells to a much greater degree than the other two, allowing more water into the network, further increasing the rate of hydrolysis and breakdown of this material. At day 40, the PL1PDA polymer has swelled approximately 400% more than either PL2PDA or PL3PDA. The PL3PDA polymer which is much less hydrophilic due to the increased PLA content initially resists swelling yielding the delay in degradation observed in Fig. 7A. The exponential nature of the swelling profiles of PL2PDA and PL3PDA in Fig. 7B is highly characteristic of cross-linked degradable hydrogel systems and has been well documented. It has been proposed that as network cross-links are degraded, the retractile forces holding the material together are weakened, allowing for greater network swelling. The amplified swelling, in turn, further increases the degree of hydrolysis of cross-links and the cyclic process compounds exponentially [17].

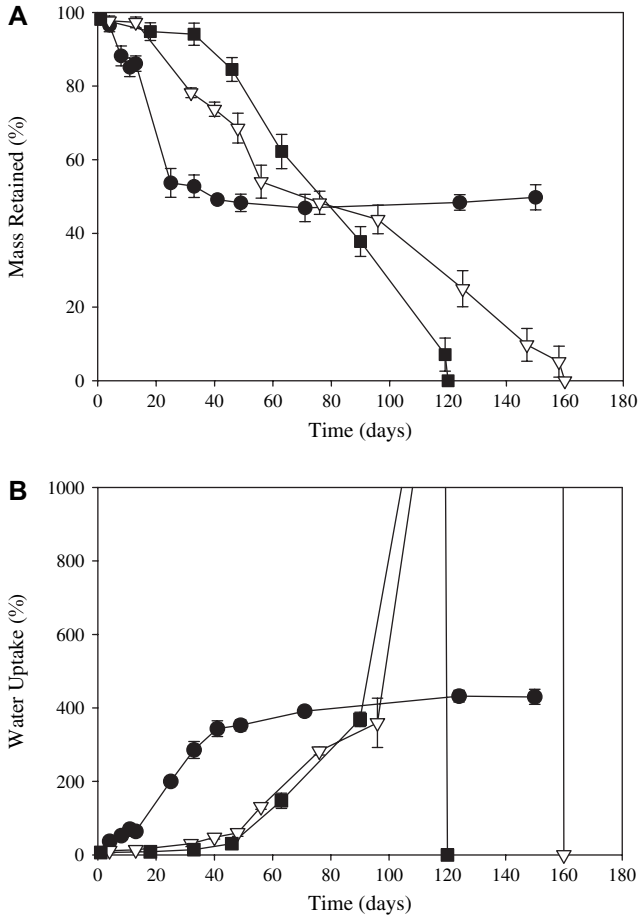

Fig. 7. (A) Degradation profiles and (B) transient swelling profiles of PL1PDA (●), PL2PDA (▽), and PL3PDA (■) fabricated with 75 wt% macromonomer in pre-polymerized formulations.

While the degree of swelling is a considerable factor in the degradation of PLPDA, other aspects in this dynamic system influence the degradation rate of these materials. For example, to degrade a cross-link in the network, water must only cleave one ester bond in the backbone of that cross-link. Therefore, macromonomers with significantly more ester groups per cross-linking backbone (i.e. PL3PDA) will have an increased probability of a water molecule finding an ester bond and breaking that cross-link. Previous studies have demonstrated an increase in degradation rate for materials with greater ester contents in their cross-linking macromonomers [14]. This behavior is also observed for the PLPDA materials in Fig. 7A, in that once each network is sufficiently swollen with water (days 70–80), the hydrophilicity no longer governs the degradation rate of the network. Instead, the amount of degradable lactide in each material determines the material's degradation rate with PL3PDA completely degrading in approximately 122 days and PL2PDA undergoing complete degradation in 160 days.

In Fig. 7A, it is observed that PL1PDA, while initially degrading very rapidly, reaches a point at 45% mass loss in which degradation seems to halt or proceed very slowly. This phenomenon is attributed to the nature of the synthesis of these materials, in which DL-lactide is expected to add to the PEGA in step one of the synthesis in a statistical manner. While it is theorized that the majority of the PL1PDA macromonomers will have one lactide per PEGA molecule, normal probability dictates that a fraction of these macromonomers will have two or more lactides per PEGA and others will have no lactide per PEGA. Furthermore, if two PEGA molecules with no added lactide are coupled in step b of the reaction (Fig. 1), a non-degrading cross-link will be created in the network. Previous work has demonstrated that as little as 2 wt% of non-degrading cross-linking monomer mixed in with a degradable polymer system is enough to induce a relatively permanent network after initial degradation mass loss

[25]. As the lactide to PEGA ratio increases in the synthesis reaction, the chances of creating a PEGA with no grafted lactide decreases significantly, resulting in a material that is fully degradable as observed with PL2PDA and PL3PDA gels.

Degradation and swelling were also tracked for PLPDA materials polymerized with 40 wt% macromonomer solutions in comparison to 75 wt% solutions. Fig. 8 describes the transient mass loss and swelling of 40 wt% PL2PDA compared to the same material polymerized at 75 wt% macromonomer loading. Due to an increase in void space and decrease in cross-link density, the 40 wt% PL2PDA swells to a much greater degree than the 75 wt% material as demonstrated earlier in Fig. 4. The decrease in cross-linking and increase in swelling has a dramatic effect on the degradation of the 40 wt% PLPDA materials, cutting the degradation time of PL2PDA to 52 days, approximately 40% of the higher macromonomer loaded PL2PDA material which degrades in 160 days. Although only the PL2PDA at 40 wt% macromonomer loading is displayed in Fig. 8, the same trends observed with the three 75 wt% macromonomer PLPDA materials (Fig. 7), i.e. decreased swelling and initial degradation with increased lactide content, are also observed with each of the 40 wt% macromonomer loaded PLPDA polymers.

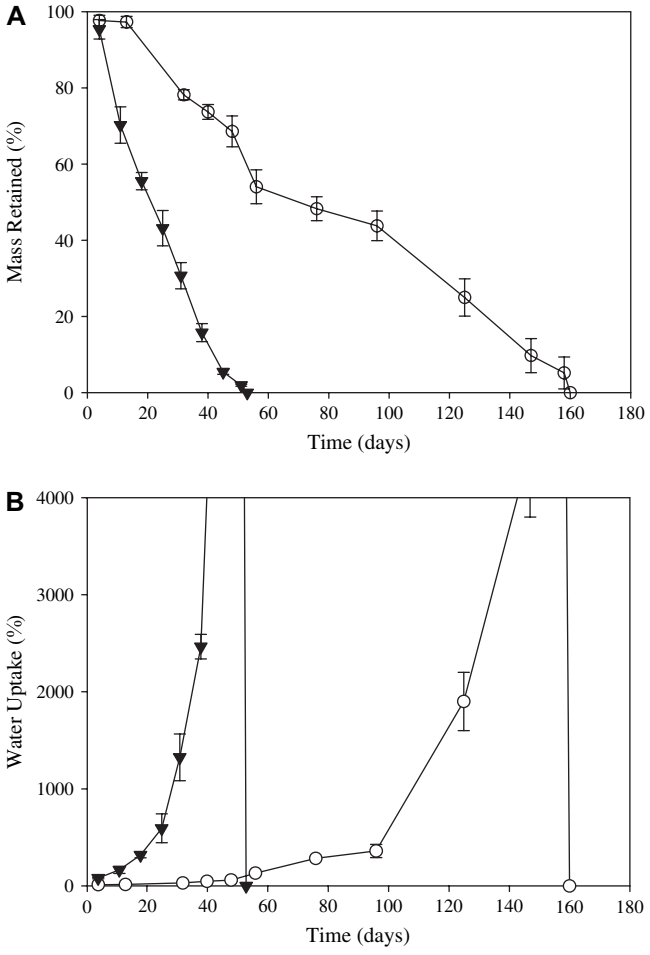

Fig. 8. (A) Degradation profiles and (B) transient swelling profiles of PL2PDA fabricated from 75 wt% macromonomer (○) and 40 wt% macromonomer (▼) in pre-polymerized formulations.

3.7. Cell biocompatibility analysis

The ultimate goal in the development of the PLPD(M)A macromonomers is to use these photopolymerized materials in biomedical applications. Therefore, it is essential to show that the synthesized materials are biocompatible, and that their degradation products are relatively non-toxic to the cells surrounding a potential implant of these materials. Cell toxicity tests were performed using a lactate dehydrogenase (LDH) assay designed to detect cell or tissue damage as a result of environmental factors. As cells undergo lysis as a result of either physical or chemical damage, they release cytoplasmic LDH in response to plasma-membrane damage. The amount of LDH released, quantified using an ELISA assay and plate reader, is therefore a good approximation of the amount of cell death that is a direct result of the polymer material present in the cell's environment. In this study, a healthy monolayer of mouse endothelial cells was cultured and then incubated with small square samples of the degrading PLPDA polymers. Cells were tested with PLPDA samples of varied lactide content, as well as samples in both the initial and mid-stages of their degradation profile.

Fig. 9 lists the relative cytotoxicity of the PLPDA materials as compared to a healthy cell culture with no polymer sample (control), as well as samples in which all the cells were lysed (100% cell death). From Fig. 9, it is observed that a decreasing amount of cell death occurs as the lactide content in the non-degraded biopolymers is increased, to the point in which PL2PDA and PL3PDA are equal or better in terms of biocompatibility to the control sample of no polymeric material in the culture. This result is not unexpected as previous work has documented that high molecular weight PLA is very biocompatible and supports cell adhesion and proliferation while PEG is a relatively inert biomaterial and does not promote protein or cell attachment [16]. By altering the PLA to PEG content of the macromonomer, the overall polymer can be made to display more PLA to the free cells, presenting a more favorable

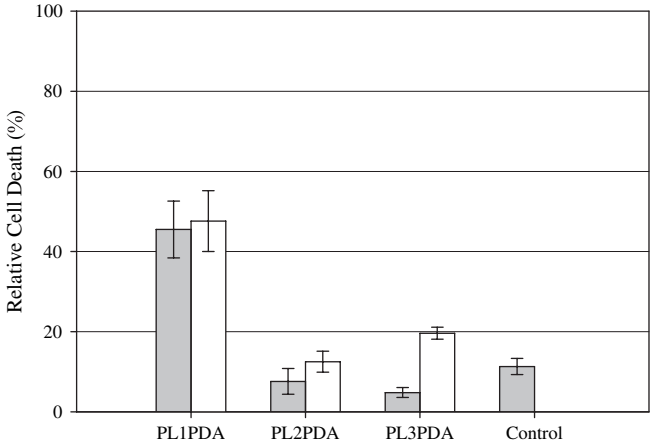

Fig. 9. Cell cytotoxicity of initial PLPDA materials (▨) as well as PLPDA polymers degraded for 2–5 weeks (□) as determined from an LDH cytotoxicity ELISA assay. The control sample represents natural cell death over the weeklong test without polymer samples present.

surface for the cells to potentially attach and proliferate, effectively making PL3PDA more biocompatible than the macromonomers synthesized with lower lactide content. Additional control tests were performed to insure that the degradation products of the polymer constructs (lactic acid) did not interfere with the LDH assay, through a reduction in enzymatic activity or through competitive binding on the LDH receptor sites, resulting in an artificial LDH reading.

In addition to the initial state biocompatibility assessment of the PLPDA materials, the LDH assay was also performed on samples with significant degradation (2, 3 and 5 weeks in solution for 75 wt% PL1PDA, PL2PDA, PL3PDA, respectively) to investigate the cytocompatibility of the biomaterials at the peak rate of their mass loss, and gauge the effect of the degradation products on the biocompatibility of the synthetic polymers. It is observed in Fig. 9 that for both PL1PDA and PL2PDA materials, little to no change in cytotoxicity occurs as the network degrades. This result strongly suggests that the degradation products, including the primary product for this portion of the mass loss profile (lactic acid), is not generated in sufficient concentrations for the PL1PDA and PL2PDA materials to have a negative effect on the growing endothelial cells. The PL3PDA materials do, however, show a slight increase in cell toxicity, approximately 15% cell death over the non-degraded material. This result is attributed to the greater lactide content in the PL3PDA network that will increase the degradation rate after week 4 (Fig. 7A) and release a greater concentration of lactic acid that could potentially decrease the pH of the medium and present an unfavorable environment to the endothelial cells.

The biocompatibility results above reinforce one of the main themes of this work, in that small changes to the PEG–PLA–PEG block composition of the synthesized macromonomer directs the overall chemistry and structure of the generated polymeric networks, and therefore have a great impact on the physical and physiological behavior of these biomaterials. By discerning and characterizing the relationships between the designed structure and chemistry of the macromonomer and the resulting behavior of the synthesized biomaterial, a significant degree of control over the physical properties of the PLPDA materials is realized. This work serves to demonstrate the highly tailorable physical behavior that is accessible with the PLPDA materials, and presents this synthetic material as a platform biopolymer that has potential towards a variety of biomedical applications.

4. Conclusions

Block macromonomers, comprising of a hydrophobic PLA biodegradable core and hydrophilic PEG ends, were enhanced to include photopolymerizable reactive groups to allow the macromonomers to form highly cross-linked, mechanically stable biopolymers. These newly synthesized cross-linked biomaterials with a reverse block structure from traditional PLA–PEG–PLA macromonomers were characterized in this study in an effort to expand their potential use in applications such as drug delivery vehicles, multi-component biocomposites, tissue engineering scaffolds, or nanostructured biopolymer systems. The results from this study indicate that by varying the PEG and PLA content in the synthesized macromonomers, many of the physical properties of the resulting polymeric materials can be directly controlled. Specifically, as the PLA content in the biomaterial is increased and the polymer is made more hydrophobic, network swelling decreases over 50%, degradation is delayed by 40 days, and the glass transition temperature is shifted approximately 15 °C. Furthermore, as the cross-link density is decreased with the addition of PLA groups in the macromonomer, the modulus of the biomaterial changes from 50 to 60%. Though the new polymeric materials are generally biocompatible, the cell compatibility of the synthesized biopolymer is also enhanced by optimizing the PEG to PLA ratio towards the more hydrophobic copolymers. The degree of control over physical and chemical properties simply by changing the PLA content in the chemical backbone of the PEG–PLA–PEG macromonomers makes this material an excellent biodegradable polymer candidate with the range and potential to serve in a variety of biomedical materials applications.

Acknowledgement

The authors would like to thank John Snyder at The University of Iowa, NMR Central Research Facilities for assistance with NMR spectroscopy. The authors gratefully acknowledge financial support from The University of Iowa through a Biosciences Initiative Grant and Presidential Fellowship, as well as support from The National Science Foundation (PECASE CBET0328231, CBET0626395), and The National Eye Institute (grant EY014563).

References

[1] Lavik E, Langer R. Appl Microbiol Biotechnol 2004;65:1–8.
[2] Wang D, Williams CG, Yang F, Elisseeff JH. Adv Funct Mater 2004;14:1152–9.
[3] Hollister SJ. Nat Mater 2005;4:518–24.
[4] Davis KA, Anseth KS. Crit Rev Ther Drug Carrier Syst 2002;19:385–423.
[5] Drury JL, Mooney DJ. Biomaterials 2003;24:4337–51.
[6] Kim BS, Mooney DJ. TIBTECH 1998;16:224–9.
[7] Lavik EB, Klassen H, Warfvinge K, Langer R, Young MJ. Biomaterials 2005;26:3187–96.
[8] Burdick JA, Chung C, Jia X, Randolph MA, Langer R. Biomacromolecules 2005;6:386–91.
[9] Butler DL, Goldstein SA, Guilak F. J Biomech Eng 2000;122:570–5.
[10] Cowin SC. J Biomech Eng 2000;122:553–69.
[11] Lieb E, Tessmar J, Hacker M, Fischbach C, Rose D, Blunk T, et al. Tissue Eng 2003;9:71–84.
[12] Li F, Li S, Vert M. Macromol Biosci 2005;5:1125–31.
[13] Lucke A, TeBmar J, Schnell E, Schmeer G, Gopferich A. Biomaterials 2000;21:2361–70.
[14] Sawhney AS, Pathak CP, Hubbell JA. Macromolecules 1993;26:581–7.
[15] Burdick JA, Philpott LM, Anseth KS. J Polym Sci Polym Chem 2001;39:683–92.
[16] Zhang K, Simon CG, Washburn NR, Antonucci JM, Lin-Gibson S. Biomacromolecules 2005;6:1615–22.
[17] Mason MN, Metters AT, Bowman CN, Anseth KS. Macromolecules 2001;34:4630–5.

[18] Metters AT, Anseth KS, Bowman CN. Polymer 2000;41:3993–4004.
[19] Clapper JD, Guymon CA. Macromolecules 2007;40:1101–7.
[20] Clapper JD, Guymon CA. Adv Mater 2006;18:1575–80.
[21] Jeong B, Bae YH, Lee DS, Kim SW. Nature 1997;388:860–2.
[22] Maleki A, Kjoniksen AL, Knudsen KD, Nystrom B. Polym Int 2006;55:365–74.
[23] Perera DI, Shanks RA. Polym Int 1996;39:121–7.
[24] Gibson SL, Jones RL, Washburn NR, Horkay F. Macromolecules 2005;38:2897–902.
[25] Bryant SJ, Anseth KS, Lee DA, Bader DL. J Orthop Res 2004;22:1143–9.
[26] Bryant SJ, Bender RJ, Durand KL, Anseth KS. Biotechnol Bioeng 2004;86:747–55.
[27] White TJ, Liechty WB, Natarajan LV, Tondiglia VP, Bunning TJ, Guymon CA. Polymer 2006;47:2289–98.
[28] Lester CL, Smith SM, Colson CD, Guymon CA. Chem Mater 2003; 15:3376–84.
[29] Sinclair J, Salem AK. Biomaterials 2006;27:2090–4.
[30] Odian G. Principles of polymerization. 4th ed. New Jersey: W&S; 2004.
[31] Brandrup J, Immergut EH, Grulke EA. Polymer handbook. 4th ed. New Jersey: W&S; 1999.
[32] Sabino MA, Ajami D, Salih V, Nazhat SN, Vargas-Coronado R, Cauich-Rodriguez JV, et al. J Biomater Appl 2004;19:147–61.
[33] Flory J. Principles of polymer chemistry. Ithaca, NY: Cornell University Press; 1953.
[34] Sperling LH, Fay JJ. Polym Adv Technol 1991;2:49–56.
[35] Kalakkunnath S, Kalika DS, Lin H, Freeman BD. Macromolecules 2005;38:9679–87.